



## **Impact of attachment pattern on the out-of-plane buckling capacity of light-gage corrugated steel decks**

Divyansh R. Kapoor<sup>1</sup>, Kara D. Peterman<sup>2</sup>, Brian Bogh<sup>3</sup>

### **Abstract**

Support attachment patterns impact the out-of-plane buckling capacity and end warping behavior of corrugated light-gage steel decks. Long span decks and decks with high fastener concentration at the sidelaps and edge supports are especially susceptible to failing in out-of-plane buckling instead of failure controlled by fastener limit states. Relevant design specifications assume that steel decks are fully attached (fastened at the bottom of each flute, –for example, a 36/7 attachment pattern) but practical construction practices often utilize reduced fastener patterns (ex – 36/5 and 36/4 attachment patterns), resulting in a detrimental impact on capacity which is neglected in the strength calculation. The out-of-plane buckling strength and reduction due to three industry-standard attachment patterns are explored by evaluating results of three AISI S907-compliant experimental tests. These tests are simulated in the commercially available finite element analysis software ABAQUS (Version 6.14) with non-linear material properties and simplified boundary conditions to estimate the buckling capacity of the test specimen. Results of the experimental and numerical study are presented along with a future experimental test matrix designed to quantify the impact of support attachment on out-of-plane panel buckling strength.

### **1. Introduction and background**

Corrugated metal panels have been widely utilized as a component in various structural applications such as bridge girders, shipping containers, airplane fuselage and wings, and metal building lateral force resisting systems due to its increased shear and out of plane buckling resistance when compared to flat sheets. In its application as a metal building lateral force system, diaphragms constructed with steel deck have been used to create floor, roof, and wall diaphragms in the structure. Typical components of a diaphragm include support connections, edge connections, sidelap connections, metal deck, and supporting framing members (Figure 1.a). The available strength of these diaphragms are controlled by the limit states of connection failure and out-of-plane buckling of the steel deck. Design guidance on these limit states is provided in AISI S310 (AISI 2016a), SDI DDM04 (Luttrell 2015), and SDI-SDCFSFDM (Sputo 2017) and while the limit state of connections is well understood, deficiencies exist in the understanding of the out-of-plane buckling limit state. Reducing support fastener attachment patterns (Figure 1.b to 1.c, 1.d) have a detrimental impact on the connection limit states (Figure 3.a) but their impact on panel

---

<sup>1</sup> Graduate Research Assistant, University of Massachusetts, Amherst, <dkapoor@umass.edu>

<sup>2</sup> Assistant Professor, University of Massachusetts, Amherst, <kdpeterman@umass.edu>

<sup>3</sup> Senior Research Engineer, Vulcraft/Vercro Group, Sacramento, <bbogh@vercodeck.com>

buckling capacity has not been investigated. Further, existing studies and calibration attempts have focused on fully attached specimen (36/7) whereas practical construction practices can often utilize reduced fastener patterns (ex – 36/5 and 36/4 attachment patterns).

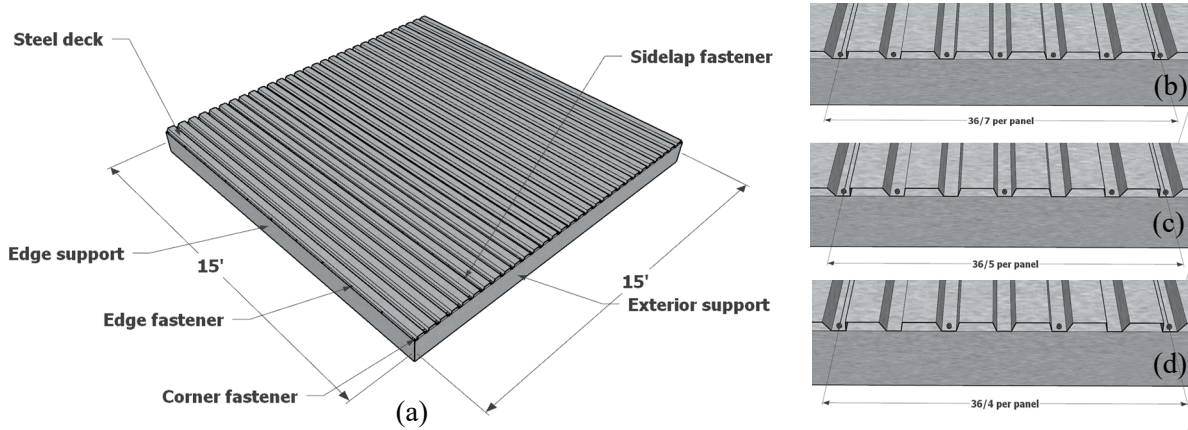


Figure 1: Typical components of a metal deck diaphragm (a) and 36/7 (b), 36/5 (c), 36/4 (d) attachment patterns

The existing buckling limit state equation (Equation 1) is a modified and calibrated form of the elastic buckling equation (Equation 2) developed by Easley and McFarland (Easley 1975). They developed elastic buckling equations to predict critical shear load per unit length of a corrugated metal panel by utilizing the Ritz energy method. Panels were treated as plates having different flexural rigidities in the two perpendicular directions and the ends were assumed to be simply supported through the bottom of every flute. These equations were validated via a suite of eight experimental tests which varied in aspect ratio, corrugation pitch, and stiffness in the orthogonal directions. Tabs attached to the mid-plane of corrugations were utilized to apply load through the neutral axis of the panel. These tabs were clamped into the test frame in an attempt to create a simply supported condition.

$$S_{nb} = \frac{7890}{\alpha L_v^2} \left( \frac{I_{xg}^3 t^3 d}{s} \right)^{(0.25)} \quad (1)$$

$$S_{nb} = 36\beta \frac{D_x^{1/4} D_y^{3/4}}{b^2} \quad (2)$$

The equation's predicted buckling capacities were within 1.06 to 1.25 of the experimentally measured capacities. Easley discovered that tabs had an end restraining effect which caused deviation from the equation as the supports no longer behaved as purely simply supported connections. The restraining effect of the tabs were accounted for by the end restraint coefficient  $\beta$  which theoretically varied between 1.0 and 1.9. They concluded that the elastic buckling equation was accurate for simply supported panels ( $\beta = 1.0$ ), but true variation of  $\beta$  with end restraint is unknown and depended upon the attachment conditions.

Nunna (Nunna 2011) evaluated the performance of panel buckling equations from TSM (Army, Navy, and Air Force 1982), SDI DDM03 (SDI 2004), Easley and McFarland's equations (Easley and McFarland 1975) and the proposed AISI S310 (AISI 2016a) equation (Equation 1). The

equations were used to predict the buckling capacities for a historical dataset comprising of twenty-eight full-scale experiments where failure mode was deck out-of-plane buckling and localized failure of fasteners did not occur. The specimens varied in corrugation depth (1.5 in specimen (26 nos.), 1-2 in specimen (1 no.), and 1- 5/8 in specimen (1 no.)), corrugation pitch – “d” (6 in (152.4 mm), 9 in (228.6 mm), and 12 in (304.8 mm)), gage – “t” (29, 22, 20, 18 and 16 gage), number of spans, and span length – “L”. All specimens were fully attached to the deck using the 36/7 attachment pattern. The strength to predicted ratios for TSM, Easley and McFarland, and proposed AISI S310 equation can be seen in Figure 2 below.

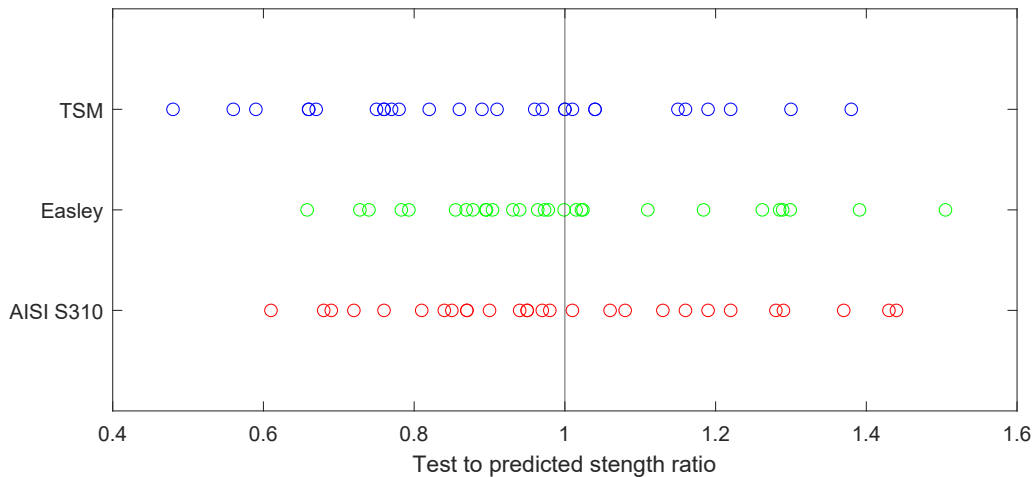


Figure 2: Performance of buckling equations from historical database (Nunna 2011)

The proposed AISI S310 equation had an average strength to predicted ratio and correlation coefficient of 1.002 and 0.910 respectively (Nunna 2011) and could be utilized for single and multi-span applications. Nunna recommended that either the TSM, modified Easley, or proposed AISI S310 equation be used for estimating the out-of-plane buckling capacity of the deck. However, there was high variability in strength to predicted ratios (0.61 – 1.44) for the proposed equation (Equation 1) and all specimens had the same fully attached 36/7 pattern.

While developing analytical models to predict strength and stiffness of profiled sheets, Wright and Hossain (Wright and Hossain 1975) also looked into the impact boundary condition attachment has on the buckling capacity of these sheets. Three distinct boundary conditions (welded through both top flat and bottom flute (Type 1), welded through bottom flute (Type 2), discretely welded with spot welds in bottom flute (Type 3)) were analyzed using finite element analysis and compared to small scale model tests. They found that Easley’s buckling equations can accurately predict shear buckling capacities but needed specific values of  $\beta$  to account for the effect of different boundary conditions i.e., end restraints. The reported  $\beta$  values varied from 1.72, 1.42, and 1.00 for Type 1, Type 2, and Type 3 boundary conditions respectively. These  $\beta$  values were back calculated from the FEA and experimental results. Further, Wright and Hossain also recommended a 50% reduction in buckling capacity if the sheets were only attached in alternate flutes. This 50% reduction also agrees with industry practice and is a significant deviation from what is recommended in codes.

This paper focuses on studying the influence of attachment pattern on the out of plane buckling capacity of corrugated steel deck. The applicable limit states and resulting design space for

common diaphragm configurations are reviewed to identify regions where panel buckling is the governing failure mode or could govern due to reduction in capacity due to the reduced attachment pattern. Results from three AISI S907 (AISI 2013) compliant diaphragm tests (Nucor 2012) are reviewed and used to calibrate the simplified finite element models. These models are then used to predict buckling capacities for the three experiments. Conclusions from the numerical study are presented along with an experimental test matrix to quantify the reduction in buckling capacity due to varying attachment patterns.

## 2. Limit states for estimation of capacity and resulting design space

The nominal in plane shear strength ( $S_n$ ) of a corrugated metal deck diaphragm is either governed by the limit state of connection failure ( $S_{nf}$ ) or the limit state of out-of-plane shear buckling ( $S_{nb}$ ). Current design standards and manuals such as AISI S310-16 (AISI 2016a) SDI DDM04 (Luttrell 2015), and SDI-SDCFSFDM (Sputo 2017) utilize the same equations for estimating these limit states. Both limit states along with some example design configurations have been discussed in the following subsections.

### 2.1 AISI S310-16 (AISI 2016a) Section D.1 – Connection limit states

The nominal shear strength per unit length of a diaphragm system when connections are the controlling limit state are further dependent on the available shear strength due to interior ( $S_{ni}$ ), corner ( $S_{nc}$ ), and edge fasteners ( $S_{ne}$ ) (Equations 3 through 5, Figure 1.a).

$$S_{ni} = [2A(\lambda - 1) + \beta] \frac{P_{nf}}{L} \quad (3)$$

$$S_{nc} = \left( \frac{N^2 \beta^2}{N^2 L^2 + \beta} \right)^{0.5} P_{nf} \quad (4)$$

$$S_{ne} = \frac{(2\alpha_1 + n_p \alpha_2) P_{nf} + n_e P_{nf}}{L} \quad (5)$$

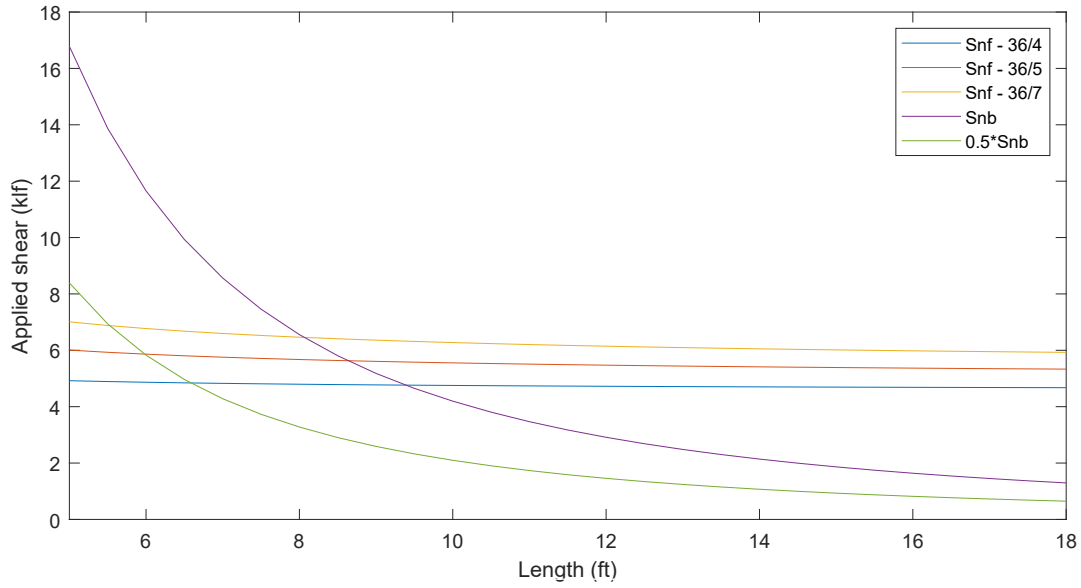
Here  $P_{nf}$  and  $P_{nfs}$  are the available shear strength of support/edge and sidelap connections respectively.  $\lambda$  is the corner connection strength reduction factor,  $\beta$  is the connection contribution and interactor factor (Note: this is different from Easley's Buckling equation end restraint  $\beta$ ),  $\alpha_1$  and  $\alpha_2$  are measures of interior and exterior support connection group distribution across a panel width ( $w_e$ ) at the edge panel.  $N$  is the number of support fasteners per panel width,  $n_p$  is the number of interior supports, and  $n_e$  is the number of edge support connections between transverse supports along the panel length.

The variation in nominal shear strength due to changing attachment pattern and span length can be seen in Figure 3.a. Fastener strength calculations were made with connection strengths from Table 1 - 36/7, specimen for a 16 gage Type B deck.

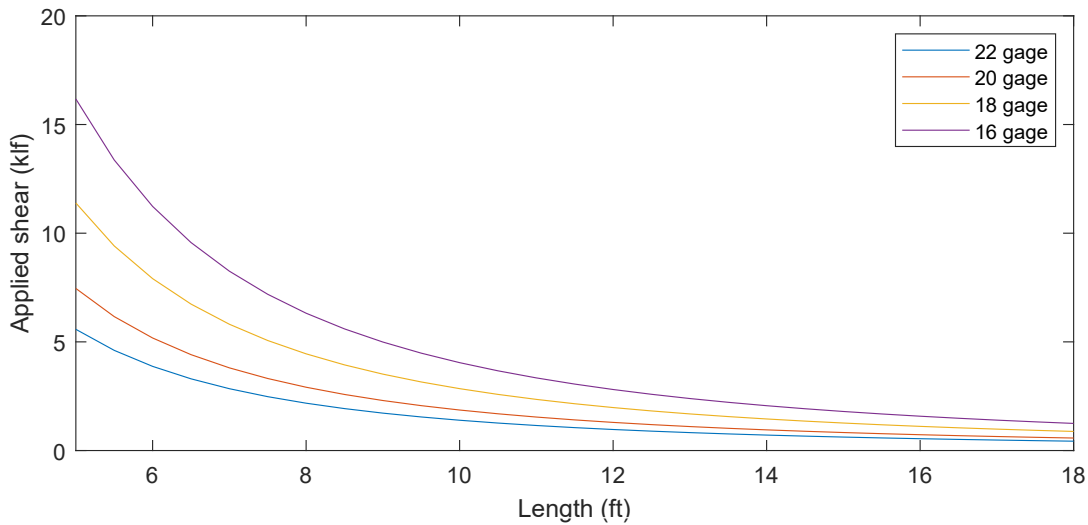
### 2.2 AISI S310-16 (AISI 2016a) Section D.2 – Stability limit, $S_{nb}$

The nominal shear strength per unit length of a diaphragm system controlled by out-of-plane buckling of the panel can be estimated using Equation 1. Here, the panel is assumed to be nearly

simply supported ( $\beta = 1.07$  (AISI 2016a)) and capacity depends upon span length ( $L_v$ ), moment of inertia ( $I_{xg}$ ), thickness ( $t$ ), corrugation pitch ( $d$ ), and the developed flute width ( $s$ ). The developed flute width is the flat width of sheet steel required to form an individual corrugation. The variation in  $S_{nb}$  due to increasing span length and gage for a Type-B deck can be seen in Figure 3.b.



(a)



(b)

Figure 3: (a) AISI S310 (AISI 2016a) Limit states for a single-span specimen  
(b) Influence of panel gage on buckling capacity

### 2.3 Reduction in critical panel length

When the attachment pattern is reduced from 36/7 to 36/4 there is a drop in the available shear capacity due to fastener limit states (Figure 3.a). However, since impact of attachment pattern is neglected in the AISI S310-16 (AISI 2016a) panel buckling limit state, the same capacity is suggested for all configurations. Panel buckling does not govern design until approximately 9.5

feet. If a 50%  $S_{nb}$  reduction curve is added to the same plot to reflect industry practice, panel buckling becomes the governing limit state earlier into the design space at 6.5 feet.

### 3. Experimental data (Nucor 2012)

To compare the available shear strength due to varying attachment patterns, results from three AISI S907 (AISI 2013) compliant cantilever tests were evaluated. These tests were part of Vercor Inc.’s Diaphragm Test Program (Test ID: 15-12, 15-14, 15-15) (Nucor 2012). The test specimen comprised of 15 feet long, 16 gage (1.5 mm thick), Type B deck, double span ( $L_v = 7.5$  feet) specimen. The attachment patterns studied were 36/7, 36/5, and 36/4. All other parameters were consistent across the tests. The yield and ultimate strength of steel was reported to be 59.4 ksi (409.5 MPa) and 73.7 ksi (508.1 MPa) respectively. Modulus of Elasticity ( $E$ ) and Poisson’s ratio ( $\nu$ ) were 29,500 ksi (203,395 MPa) and 0.3. The geometry of the deck was typical of Type B deck and individual corrugation dimensions can be seen in Figure 4 below. Inside bend radius was measured to be 0.1875 in (4.763 mm). The resulting out-of-plane buckling capacity of this deck was estimated to be 7.57 klf (110.48 KN/m) from Equation 1.

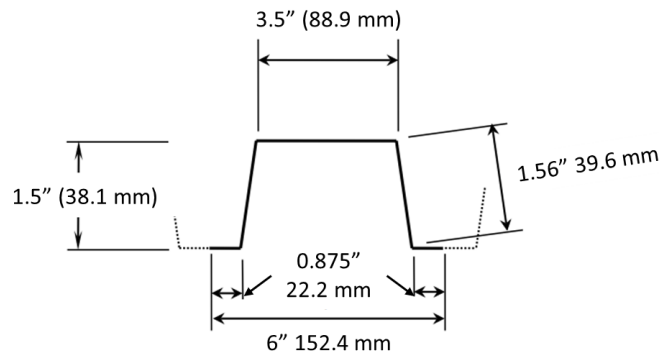


Figure 4: Individual flute geometry

Support and edge connections were made with spot ( $d = 0.90$  in) and arc seam welds ( $d = 0.385$  in and  $L_w = 1.18$  in) respectively. Edge connections were spaced 6.00 in (152.4 mm) on center along the fixed edge. There was a variation (Table 1) in both types of weld connection strengths across the tests due to variation in the effective weld diameter ( $d_e$ ) and average arc seam weld length ( $L_w$ ). This difference was accounted for in the connection limit states calculations for each configuration by adjusting the calculated weld strength, ( $P_{nf}$  &  $P_{nfe}$ ), from AISI S100 Section J2.2 and J2.3 (AISI 2016b) Sidelap connections were made with a proprietary fastening method and were placed 12 in (304.8 mm) on center along the panel junctions. The shear strength of sidelaps was 5.92 kips and was consistent across tests. Resulting connection limit states strengths, observed ultimate strength ( $S_u$ ), and failure modes for the test configurations can be seen in Table 1 below.

Table 1: Summary of experimental results

Test No.	Attachment Pattern	$S_{nf}$	$S_u$	Failure mode
		klf (KN/m)	klf (KN/m)	
15-12	36-7	6.67 (97.34) <sup>1</sup>	7.19 (104.93)	Out-of-plane buckling of deck with some pre-peak weld fractures
15-14	36-5	6.05 (88.29) <sup>2</sup>	5.82 (84.94)	Out-of-plane buckling of deck
15-15	36-4	5.31 (77.50) <sup>3</sup>	5.27 (76.91)	Deck tearing around welds at supports

- 
1. P<sub>nf</sub> = 7.46 kips (33.2 KN) & P<sub>nfe</sub> = 6.88 kips (30.60 KN)
  2. P<sub>nf</sub> = 7.87 kips (35.0 KN) & P<sub>nfe</sub> = 6.97 kips (31.0 KN)
  3. P<sub>nf</sub> = 8.22 kips (36.6 KN) & P<sub>nfe</sub> = 7.12 kips (31.7 KN)
- 

The governing failure mode in test 15-12 and 15-14 were out of plane buckling of the steel deck. In test 15-12, pre-peak weld fractures were observed which impacted the ultimate capacity of the specimen. Due to connection failure early in the test, the full AISI S310 (AISI 2016a) predicted capacity was not achieved in this test. Test 15-14 failed in pure out of plane buckling capacity of the test with no weld or deck failures. Test 15-15 failed due to tearing of deck around the welds which also limited the capacity of the test. The specimen ultimately buckled but this was after initiation of tearing which prevented the specimen from gaining any strength.

#### **4. FEA investigation**

The three experimental test configurations discussed in Section 3 were numerically simulated in the commercially available finite element software ABAQUS version 6.14 to develop simplified models that can accurately predict the ultimate capacity of the tests. Only the 15 feet x 15 feet (4572 mm X 4572 mm) deck assembly comprising of 5 individual 3 feet (914.4 mm) wide panels was modelled. Boundary conditions were simplified to localized displacements and connections were assumed to be perfectly rigid and of infinite strength. The following sections discuss this modelling methodology, its limitations, and results.

##### **4.1 Geometry, material properties, and interactions**

Individual panels with corrugation dimension from Figure 4 and thickness  $t = 0.0582$  in (1.48 mm) were modelled in the software. A linear elastic and linear strain hardening plasticity (bilinear) material model was utilized to simulate the mechanical properties of the steel. The yield and ultimate strength of steel was set to 59.4 ksi (409.5 MPa) and 73.7 ksi (508.1 MPa) respectively and a 10% elongation at failure was assumed. Sidelap fasteners were neglected in the models and the vertical flat portion of each edge flute in a panel was tied to the subsequent panel using the built-in tie constraints (Figure 5.a). The bottom flat of the first panel was tied to a reference point, RP1, located at its geometric center (Figure 5.b) using the built in MPC beam constraint.

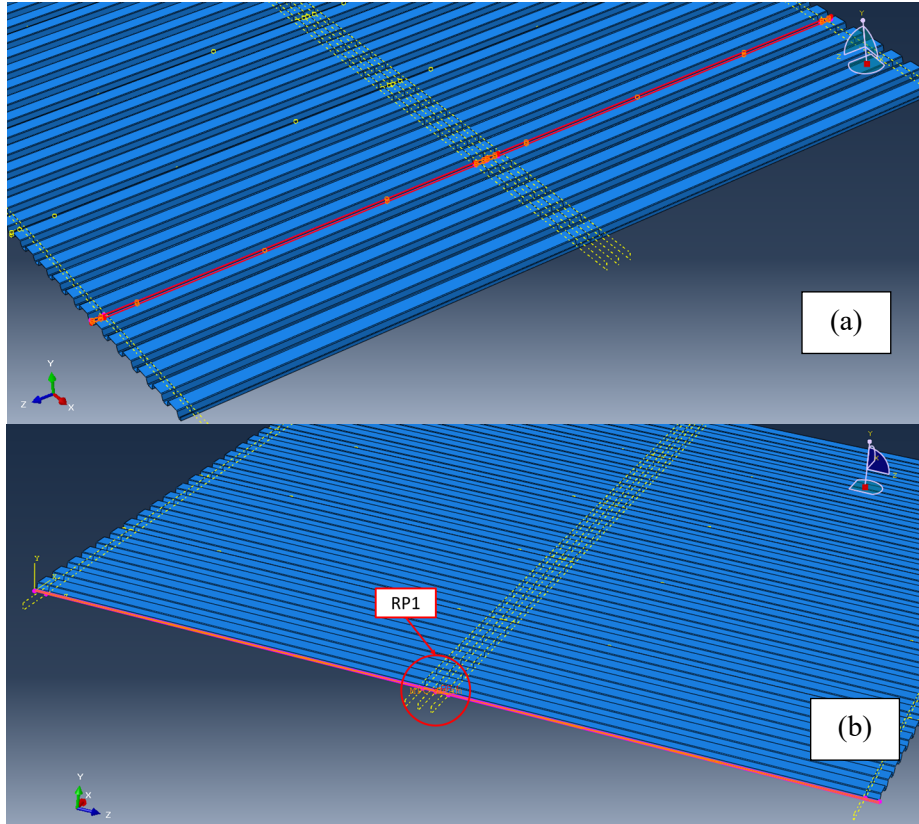


Figure 5: Sidelap (a) and edge support connection (b) idealization

#### 4.2 Meshing, boundary conditions/loading, and analysis settings

The FEA mesh used to discretize the panels can be seen in Figure 6 below. The mesh comprised of linear quadrilateral S4R shell elements, and their size varied along the length of the panel. Finer mesh was utilized at the panel ends and interior support and element size was increased in the intermediate zones to increase computational efficiency. Element sizes were varied and found to have negligible impact on the strength prediction of the model. A static general load step with non-linear geometry and automatic stabilization (default damping factor = 0.0002) was used to analyze the models.

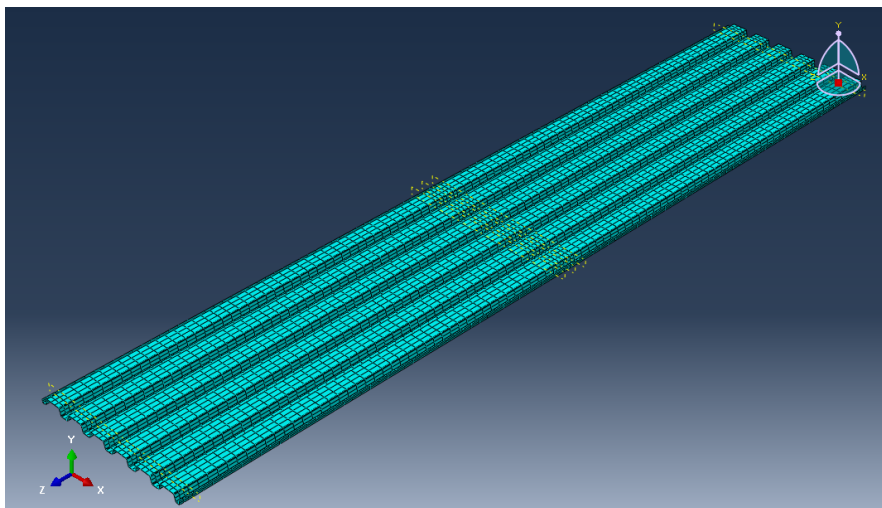


Figure 6: FEA mesh utilized in analysis

The reference point of the MPC beam constraint, RP1, was fixed ( $U1 = 0, U2 = 0, U3 = 0, UR1 = 0, UR2 = 0, UR3 = 0$ ) and used to measure the applied load in the model. Support fasteners were not explicitly modelled in ABAQUS and displacement boundary conditions were utilized to simulate the effect of welding the panels to a rigid frame. Equivalent in-plane displacements due to the motion of the test frame were calculated at each weld location and applied to the attachment points as a displacement boundary condition (Figure 7). The support attachment points were located at the bottom of each fastened flute and extended a distance of  $2d$  ( $d =$  visible diameter of weld) beyond the edges of the panel to meet minimum edge and clear distances as recommended in Section J2.2.1, AISI S100. Interior support attachment points were also assumed to be  $2d$  wide along the length of the panel. All attachment points were assumed to be as wide as the flat portion of each flute effectively clamping the entire bottom flute. The advantage and limitations of applying boundary conditions in this manner to simulate loading have been discussed in the following paragraph.

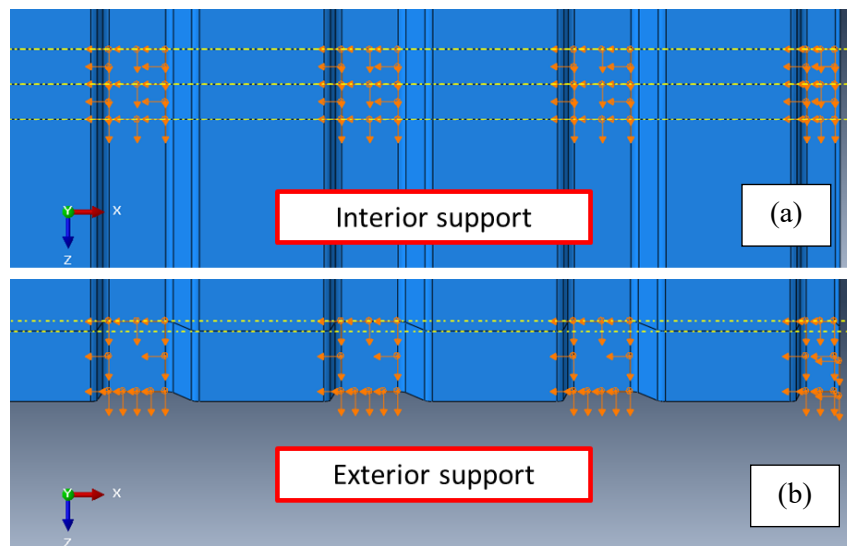


Figure 7: Interior (a) and exterior (b) support boundary conditions

By directly applying displacements at the support locations, we eliminated material and connection limit states such as deck tearing (Test ID 15-15) and weld fractures (Test ID – 15-12) which were observed in the experiments. This allowed the models to bypass these failure modes and predict panel buckling capacities based solely on panel geometry, material property, and attachment pattern end restraint. However, by directly applying rigid-frame equivalent displacements at each attachment point, flexibility of the welds and surrounding regions were completely eliminated as no localized deformations could occur. Further, connection failures could not be detected in the model since no failure criteria could be defined. Hence, redistribution after yielding of supports or failure of welds did not occur in the models and all connections continued to load the model throughout the numerical run.

### 4.3 Results and comparison with available experimental data

The force vs lateral displacement curves for the three simulations can be seen in Figure 8 below. In each of the simulations, the failure mode observed was out-of-plane buckling of the steel deck (Figure 9). Since a direct comparison of simulated results was not possible with the 36/4 (ID: 15-15) and 36/7 (ID: 15-12) experiments, results from the 36/5 experimental test (ID: 15-14) were

used to evaluate the buckling prediction of the models. For this model, the FEA predicted vs experimental capacity ratio was 1.06 (Table 2) which was deemed reasonable for the simplified model. Table 2 summarizes capacity comparisons for FEA, experimental, and AISI S310-16 predicted strengths for all three experiments.

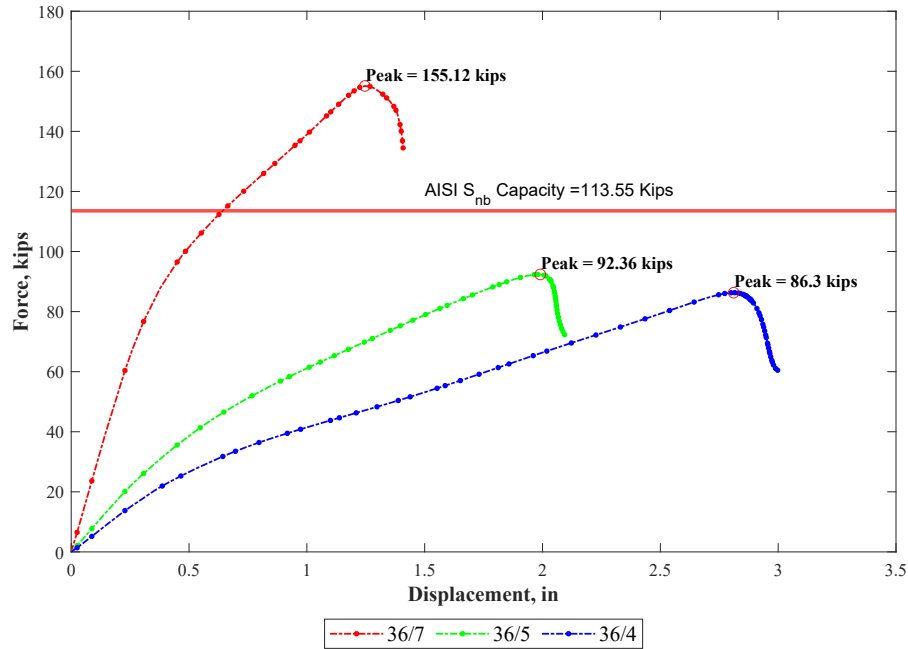


Figure 8: Finite element analysis (FEA) simulation force-displacement curves

Further, the force-displacement curve for the 36/4 FEA model followed the experimental curve up until the point of material failure in the actual test (Ripping of deck around welds). Beyond this, the simulation continued to gain strength and buckled at 86.3 kips (379.5 KN). This was 8.7% (Table 2) higher than the experimental value due to the change in failure mode.

The fully attached model predicted a capacity of 155.12 kips (690.0 KN) which was significantly higher than both the experimental (107.8 kips (479.5 KN)) and code predicted value (113.5 kips (504.9 KN)). The FEA to experimental strength ratio was 1.44 and FEA to code prediction strength ratio was 1.37 (Table 2). By comparing the FEA strength with code predicted strength (assumed  $\beta = 1.07$ ), the diaphragm end restraint coefficient was calculated to be 1.47. This is within the theoretical range of  $1.00 \leq \beta \leq 1.90$  where 1.00 corresponds to the simply supported condition. The FEA observed  $\beta$  also agrees with variation in  $\beta$  in the Historical Database in Figure 2 (Nunna 2011) and  $\beta$  observed for Type 2 boundary conditions by Wright and Hossain (Wright and Hossain 1977) which was found to be 1.42.

Table 2: Proposed experimental test matrix and resulting limit state capacities

Test No.	Attachment Pattern	$S_n$	$S_u$	$S_u$	$S_u$ (Nucor 2012)/ $S_n$ (AISI 2016a)	$S_u$ (FEA)/ $S_{nb}$ (AISI 2016a)	$S_u$ (FEA)/ $S_n$ (Nucor 2012)
		(AISI 2016a)	(Nucor 2012)	(FEA)			
		klf (KN/m)	klf (KN/m)	klf (KN/m)			
15-12	36-7	6.67 (97.34)	7.19 (104.93)	10.34 (150.90)	1.08	1.37	1.44
15-14	36-5	6.05 (88.29)	5.82 (84.94)	6.16 (89.90)	0.96	0.81	1.06
15-15	36-4	5.31 (77.50)	5.27 (76.91)	5.75 (83.91)	0.99	0.76	1.09

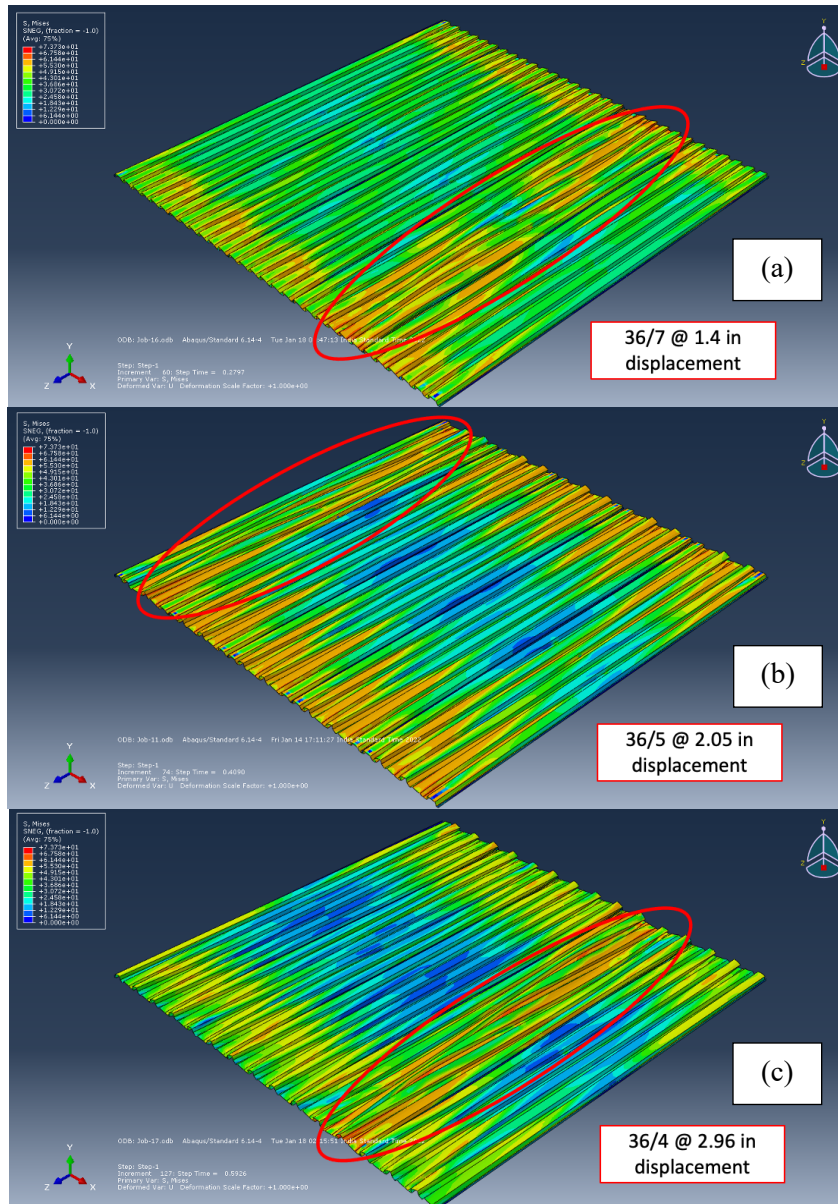


Figure 9: FEA deformed shape and stress distribution right after initiation of buckling for: (a) 36/7 (b) 36/5 (c) 36/4

## 5. Conclusions

To study the impact of attachment pattern on end restraint and out of plane buckling capacity of corrugated metal decks, three experimental tests were simulated numerically. The models utilized non-linear material properties, measured geometry, simplified boundary conditions, and excluded non-buckling related failure modes. The results from this study indicate the following:

- Attachment pattern impacts end restraint coefficient and thereby the buckling strength of the steel panel. When the simulated attachment pattern was changed from 36/7 to 36/5 and 36/4, the capacity dropped to 60% and 56% respectively for this end restraint condition
- The reduction in capacity agrees with current industry practice and literature recommendation of 50% reduction for skip patterns however design codes assume all attachment patterns have the same buckling capacity

- Fully identical experimental tests that only differ in attachment pattern and have the same failure mode are required to quantify this impact and exclude other parameters that can lead to variations in the measured strength
- Simplified high efficiency models such as the one utilized in this paper can accurately capture strength when the failure mode is buckling

## 6. Future works – Experimental test matrix

Table 3 below summarizes the planned test matrix for the AISI S907 (AISI 2013) compliant cantilever tests. The single span 15-foot-wide diaphragms will be constructed from 15-foot-long, 1.5 inch deep, 22 gage Type B deck panels. Support, edge, and sidelap connection will be made with #14 fasteners ( $P_{nfs} = 1.26$  kips). Support attachment patterns will vary from 36/4, 36/5, and 36/7 to capture a range on standard industry patterns. Each test will be repeated thrice for a total of nine tests. Predicted capacities for these specimens can be seen in Table 3. These were calculated with nominal material properties for steel and fastener strengths are based on SDI-SDCFSFDM (Sputo 2017) Section 6, Fastener and Framing tables. The tests are designed to have at least 50% greater predicted connection limit states capacity than buckling capacity to avoid connection failures during the test.

Table 3: Proposed experimental test matrix and resulting limit state capacities

No.	Support Fastener	Fastener spacing	Panel length	$L_v$	$S_{ni}$	$S_{nc}$	$S_{ne}$	$S_{nb}$
		in	ft	ft	klf	klf	klf	klf
1	36/4	6.00	15.00	15.00	1.47	0.97	2.57	0.63
2	36/5	6.00	15.00	15.00	1.53	1.15	2.63	0.63
3	36/7	6.00	15.00	15.00	1.55	1.35	2.69	0.63

## Acknowledgements

The writers gratefully acknowledge the financial support provided by the American Iron and Steel Institute (AISI) standards council, and in-kind material donations from Canam Steel Corporation and Vulcraft Verco Group.

## References

- AISI. (2013). “Test standard for cantilever test method for cold-formed steel diaphragms, (AISI S907).” American Iron and Steel Institute
- AISI. (2016a). “North American standard for the design of profiled steel diaphragm panels, (AISI S310-16).” American Iron and Steel Institute
- AISI. (2016b). “North American specification for the design of cold-formed steel structural members, (AISI S100).” American Iron and Steel Institute
- Army, Navy and Air Force. (1982) “Seismic design for buildings, (Tri-services Manual). Report No. Army TM 5-809-10.” Washington, D.C.: U.S. Government Printing Office
- ABAQUS, Version 6.14. (2014) Dassault Systèmes Simulia Corp.
- Easley, J.T. (1975). “Buckling formulas for corrugated metal shear diaphragms.” *Journal of the structural division*, 101, 1403-1417.
- Luttrell, L.D. (2004). “Diaphragm Design Manual, 3rd Edition (DDM03).” Steel Deck Institute
- Luttrell, L.D. (2015). “Diaphragm Design Manual, 4th Edition (DDM04).” Steel Deck Institute
- Nunna, R, V. (2011). “Buckling of profiled steel diaphragms” Center for Cold-Formed Steel Structures Library. 163
- Nucor. (2012). Verco Decking Inc. – Diaphragm Test Program (Test IDs: 15-12, 15-14, 15-15). Nucor, Charlotte, North Carolina
- Sputo, T. (2017). Steel Deck on Cold-Formed Steel Framing Design Manual, 1st Edition.” Steel Deck Institute
- Wright, H. D., Hossain, K.M. (1977). “In-plane shear behavior of profiled steel sheeting” *Thin-Walled Structures*, Elsevier, 29 (1-4) 79-100.